

RESEARCH ARTICLE

Nucleus pulposus structure and function assessed in shear using magnetic resonance elastography, quantitative MRI, and rheometry

Megan Co¹ | Brian Raterman² | Brett Klamer³ | Arunark Kolipaka² | Benjamin Walter^{1,4} 

¹Department of Biomedical Engineering, The Ohio State University, Columbus, Ohio, USA

²Department of Radiology, The Ohio State University Wexner Medical Center, Columbus, Ohio, USA

³Department of Biomedical Informatics, Center for Biostatistics, The Ohio State University, Columbus, Ohio, USA

⁴Department of Orthopaedics, The Ohio State University Wexner Medical Center, Columbus, Ohio, USA

Correspondence

Benjamin Walter, Department of Biomedical Engineering, The Ohio State University, 140 W 19th Ave Room 2124, Columbus, OH 43210-1132, USA.

Email: walter.367@osu.edu

Funding information

National Institute of Arthritis and Musculoskeletal and Skin Diseases, Grant/Award Number: R01AR075062

Abstract

Background: In vivo quantification of the structure–function relationship of the intervertebral disc (IVD) via quantitative MRI has the potential to aid objective stratification of disease and evaluation of restorative therapies. Magnetic resonance elastography (MRE) is an imaging technique that assesses tissue shear properties and combined with quantitative MRI metrics reflective of composition can inform structure–function of the IVD. The objectives of this study were to (1) compare MRE- and rheometry-derived shear modulus in agarose gels and nucleus pulposus (NP) tissue and (2) correlate MRE and rheological measures of NP tissue with composition and quantitative MRI.

Method: MRE and MRI assessment (i.e., T1 ρ and T2 mapping) of agarose samples (2%, 3%, and 4% (w/v); $n = 3\text{--}4/\%$) and of bovine caudal IVDs after equilibrium dialysis in 5% or 25% PEG ($n = 13/\text{PEG}\%$) was conducted. Subsequently, agarose and NP tissue underwent torsional mechanical testing consisting of a frequency sweep from 1 to 100 Hz at a rotational strain of 0.05%. NP tissue was additionally evaluated under creep and stress relaxation conditions. Linear mixed-effects models and univariate regression analyses evaluated the effects of testing method, %agarose or %PEG, and frequency, as well as correlations between parameters.

Results: MRE- and rheometry-derived shear moduli were greater at 100 Hz than at 80 Hz in all agarose and NP tissue samples. Additionally, all samples with lower water content had higher complex shear moduli. There was a significant correlation between MRE- and rheometry-derived modulus values for homogenous agarose samples. T1 ρ and T2 relaxation times for agarose and tissue were negatively correlated

Abbreviations: FOV, field of view; GAG, glycosaminoglycan; IVD, intervertebral disc; LBP, low back pain; MRE, magnetic resonance elastography; PEG, polyethylene glycol; PFA, principal frequency analysis; SE-EPI, spin-echo echo-planar imaging; SLS, standard linear solid; sTR, shot repetition time; TE, echo time; TR, repetition time; TSL, spin-lock time.

This is an open access article under the terms of the [Creative Commons Attribution-NonCommercial](https://creativecommons.org/licenses/by-nc/4.0/) License, which permits use, distribution and reproduction in any medium, provided the original work is properly cited and is not used for commercial purposes.

© 2024 The Authors. *JOR Spine* published by Wiley Periodicals LLC on behalf of Orthopaedic Research Society.

with complex shear modulus derived from both techniques. For NP tissue, shear modulus was positively correlated with GAG/wet-weight and negatively correlated with %water content.

Conclusion: This work demonstrates that MRE can assess hydration-induced changes in IVD shear properties and further highlights the structure–function relationship between composition and shear mechanical behaviors of NP tissue.

KEYWORDS

intervertebral disc, magnetic resonance elastography, shear properties

1 | INTRODUCTION

Low back pain (LBP) has been a leading cause of disability worldwide with over half a billion cases reported in 2020.¹ LBP has been associated with intervertebral disc (IVD) degeneration which is characterized by a progressive breakdown in structure and results in loss of mechanical function. Previous studies have observed an increase in *in vitro* IVD compressive and shear modulus with degeneration via mechanical testing.^{2–5} These studies suggest that with aging and/or progressive degeneration, the IVD's ability to fulfill its primary mechanical role of load support and flexibility within the spine becomes compromised. These *in vitro* results suggest that assessing IVD mechanics *in vivo* could facilitate studying the changes in mechanical properties in physiological conditions and could also measure the subtle changes that may be present in earlier stages of IVD degeneration. The *in vivo* measurements can be correlated with its current structure as composition and mechanical function have been seen to be closely linked. Therefore, there is a need for quantitative imaging techniques that will assess the mechanical behavior and composition of the IVD *in vivo*.

Magnetic resonance elastography (MRE) is an imaging technique capable of assessing changes in shear mechanical properties with disease and has been applied to a variety of soft tissues including the heart, brain, and liver.^{6–10} Multiple studies have utilized MRE on the IVD and demonstrated its potential to assess disease-related changes in shear properties^{11–16}; However, it remains unclear how representative MRE measures of IVD shear modulus are compared with those derived from torsional mechanical testing. MRE-derived measurements have been compared with those derived from rheometry in the liver where there is ample tissue for both MRE and rheological assessment and demonstrated good agreement between techniques.¹⁷ Multiple studies have assessed the changes in mechanical properties of nucleus pulposus (NP) tissue with degeneration via shear testing^{4,18,19}; however, few studies have made the direct comparison to MRE-derived mechanical properties. This study aims to directly compare shear properties derived from MRE and rheometry at similar frequencies.

Quantitative MRI techniques, such as T1p and T2 mapping, have been used to inform IVD composition as they have been seen to correlate with glycosaminoglycan (GAG) and water content.²⁰ Given that the composition and organization of the extracellular matrix directly impacts the mechanical function of the tissue, quantification

of GAG and water content via T1p and T2 mapping, respectively, may help inform the degeneration process *in vivo*. Additional studies have then demonstrated that these quantitative MRI metrics correlate with functional compressive properties, suggesting that T1p and T2 mapping can inform changes in mechanical properties of IVDs in early or advanced stage degeneration.^{21,22} However, the structure–function relationship as quantified via T1p and T2 and their association with shear properties remains unclear. Focusing on the IVD's response to shear loading may inform the mechanical behavior of the tissue based more on the organization of extracellular matrix with water influencing the solid interactions as opposed to compressive loading where fluid flow plays a larger role in the tissue's mechanical response. Therefore, the objectives of this study were to (1) compare MRE-derived and rheometry-derived shear modulus in both homogenous agarose gels and NP tissue and (2) correlate MRE and rheological measures of NP tissue with composition and quantitative MRI.

2 | METHODS

2.1 | Agarose preparation/testing

For initial agarose validation, multiple batches of 2% ($n = 4$), 3% ($n = 3$), and 4% ($n = 3$) (w/v) agarose were created to provide a spectrum of hydrated gels. From a singular batch, samples were cast for MRI and mechanical testing. The 2%, 3%, and 4% agarose samples were cast in a $\sim 120 \text{ mm} \times 120 \text{ mm} \times 30 \text{ mm}$ plastic container for MRI scans. The 2% agarose samples contained embedded IVD tissue which is further explained in Section 2.2 IVD tissue preparation. For mechanical testing, agarose samples (20 mm $\varnothing \times 1.5 \text{ mm}$ thick) were cast on electrophoresis plates (Bio-Rad) to ensure uniform thickness and a cylindrical plug was punched out. Three replicates of agarose plugs were created/tested from a singular batch. A schematic of the mechanical testing setup with the geometry of the agarose sample is shown (Figure 1C).

2.2 | IVD tissue preparation/testing

Sixteen bovine tails were obtained from a local abattoir from which a total of 26 IVDs were isolated from the C1/2 or C2/3 level. The hydration of the IVDs was altered via equilibrium dialysis to provide a

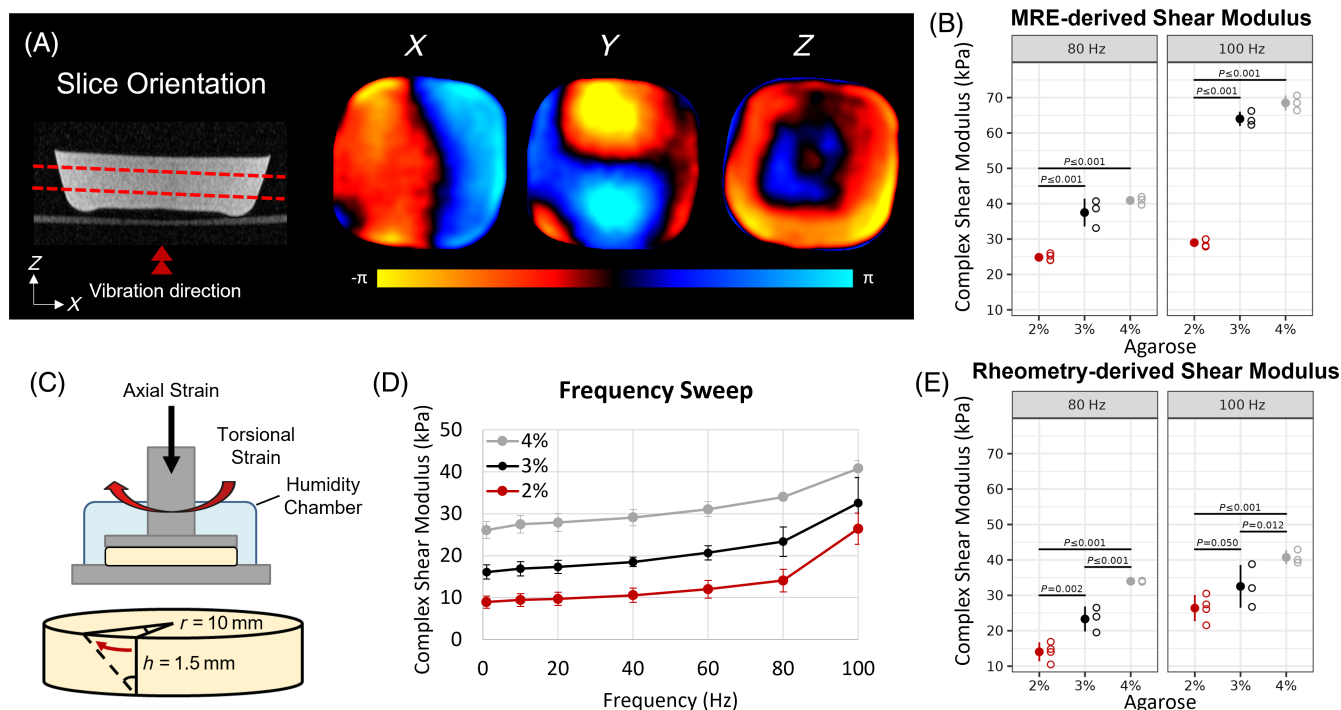


FIGURE 1 Agarose shear properties validation: (A) Schematic of slice orientation through T2-weighted scan of agarose sample with wave propagation in the x, y, and z direction. (B) Comparison of shear modulus derived from MRE between 2% ($n = 4$), 3% ($n = 3$), and 4% ($n = 3$) agarose at 80 and 100 Hz. (C) Schematic of agarose sample undergoing torsional shear testing using a rheometer. (D) Dynamic frequency sweep results for all agarose samples at a shear strain amplitude of $\gamma_0 = 0.05\%$ at frequencies ranging between 1 to 100 Hz. (E) Comparison of shear modulus derived from rheometry between all agarose samples at 80 and 100 Hz.

range of tissue with different mechanical properties. Whole discs with the endplates removed were sealed in dialysis tubing (cutoff 1 kDa, Sigma-Aldrich) and placed in one of two osmotic conditions: 5% ($n = 13$ IVDs) or 25% ($n = 13$ IVDs) (g/mL) polyethylene glycol (PEG) (20 kDa, Sigma-Aldrich) in 0.15 mol/L NaCl exerting an osmotic pressure of 0.027 or 0.565 MPa, respectively.²³ The swelling pressure of the IVD was forced to match the osmotic pressure of the solution causing the tissue to absorb (5% PEG) or lose water (25% PEG). After ~ 40 h at room temperature, the discs were removed, vacuum sealed in plastic bags, and embedded in 2% agarose for MRI scanning. After completion of MRI scans, the NP region was dissected from the whole disc and frozen at -20°C . Tissue samples for mechanical testing (8 mm $\varnothing \times 2$ mm thick) were then prepared using a cryostat microtome (Tissue-Tek Cryo₃ Flex, Sakura, Torrance, CA) as previously described.²⁴ Briefly, tissue was sectioned to a thickness of 2 mm, an 8-mm biopsy punch was used to extract the plugs, and the wet weight of the plugs were recorded. A schematic of the mechanical testing setup with the geometry of the NP tissue plug is shown (Figure 3C).

2.3 | MRI image acquisition and analysis

All imaging was performed using a 3T MRI scanner (Prisma, Siemens Healthcare, Erlangen, Germany). Mechanical excitation was applied to the bottom of the agarose container (Figure 1A). Vibration waves

were similarly applied to the bottom of the agarose container containing the IVDs (Figure 3A). For both agarose and NP tissue, a gradient recalled echo based T1p mapping sequence was used to acquire one transverse slice with the following parameters: spin-lock frequency = 500 Hz, sTR (shot repetition time) = 2642 ms, TSL (spin-lock time) = 10, 20, 30, ..., 340 ms, TR (repetition time) = 9.3 ms, TE (echo time) = 4.4 ms, field of view (FOV) = 200×200 mm, slice thickness = 2 mm, acquisition matrix = 192×192 , averages = 3. A spin-echo based T2 mapping sequence was used to acquire a transverse slice with the following parameters: TE = 8, 16, 24, ..., 256 ms, TR = 2000 ms, FOV = 200×200 mm, slice thickness = 2 mm, acquisition matrix = 192×192 , averages = 2. For IVD tissue, a region of interest (ROI) of the NP region was hand drawn (MC with 5 years' experience in spine research) based on the respective anatomical T2-weighted transverse scans and superimposed onto all T1p and T2 images. Relaxation values were determined by fitting signal intensity values to an exponential decay, $S_i = S_0 \times \exp(-\text{TSL}/\text{T1p}) + C$ or $S_i = S_0 \times \exp(-\text{TE}/\text{T2}) + C$ where S is the signal intensity, TSL is the spin-lock time, TE is the echo time, and C is a constant, using a custom MATLAB code (version 2018b Mathworks, Natick, MA). A 3×3 pixel kernel median filter and 95 percentile cutoff was applied to all T1p and T2 maps.

A spin-echo echo-planar imaging (SE-EPI) MRE sequence at 80 and 100 Hz was used to assess shear modulus. 80 Hz was utilized as previous studies have performed MRE on IVDs at that frequency

for adequate wave penetration and wavelength estimation.^{15,16} 100 Hz was utilized as a point of comparison and because it was the highest frequency within the limits of both the MRE driver and rheometer. SE-EPI sequences capturing individual (SE-EPI_i/n = 20 IVDs) or multiple (SE-EPI_m/n = 6 IVDs) discs embedded within agarose were used with slight differences in parameters based on the different number of slices. Scans of NP tissue and the surrounding agarose it was embedded within using the SE-EPI_i sequence consisted of two or three, 1 mm, contiguous transverse slices (dependent on disc height) acquired within a single TR using a previously described SE-EPI MRE sequence.²⁵ Slice locations were chosen to encompass as much of the NP region as possible. Additional SE-EPI_i parameters: FOV = 120 × 120 mm, TE = 30.40 ms, TR = 900 ms, acquisition matrix = 128 × 64, averages = 14, GRAPPA 2. The SE-EPI_m sequence consisted of 30 × 0.8 mm slices encompassing all discs. Additional SE-EPI_m parameters: FOV = 120 × 120 mm, TE = 31.30 ms, TR = 2250 ms, acquisition matrix = 128 × 64, averages = 22, GRAPPA 2. For IVD tissue, ROI of the NP region was hand drawn (MC with 5 years' experience in spine research) based on the MRE magnitude images and superimposed onto all phase images. The average shear modulus estimates for the NP region was calculated using a modified principal frequency analysis (PFA) method described previously.^{15,26} Briefly, filtering was performed to remove noise and reflected waves via a fourth order Butterworth bandpass filter applied in eight directions with cutoff values 1–40 waves/FOV. The 3D PFA was performed in all three encoding directions to obtain weighted shear modulus value.

2.4 | Mechanical testing and NP tissue hydration/GAG analysis

All mechanical testing was performed using a Discovery HR-2 rheometer (TA instruments, New Castle, DE) with a custom humidity chamber to minimize dehydration. Sandpaper (120 grit) was attached to the upper and lower platen to minimize sample slippage. To determine the initial height of the sample, the upper platen was lowered until a compressive preload of 0.1 N was obtained. The gap at the initial height (i.e., after the pre-load had been achieved) was used to apply an axial strain of 10% over 10 s which was held for 300 s. After reaching compressive equilibrium, a frequency sweep was performed from 1 to 100 Hz at a rotational strain of 0.05%. A 0.05% strain was determined to be within the linear viscoelastic region from amplitude sweep tests from 0.01% to 1% strain (Figure S1). For NP tissue, additional creep and stress relaxation tests were performed for further quantification of mechanical properties via the standard linear solid (SLS) viscoelastic model. For creep testing, a torsional stress of 0.05 kPa was applied and held for 180 s while the strain response was recorded. Immediately after, the stress was removed, and the tissue was allowed to relax for 180 s before the stress relaxation test. A torsional strain of 10% was then applied over 1 s and held for 600 s while the shear stress relaxation response was recorded. Subsequently, the tissue plugs were lyophilized to obtain dry weight. Water content was calculated as a percentage of wet weight, (wet

weight – dry weight)/wet weight × 100%. After lyophilization ~5 mg of dry tissue was digested with proteinase K, and the GAG content of all samples was assessed via the DMMB assay as previously described.²⁷ The GAG content from the NP region of three fresh (non-equilibrated) IVDs was also obtained to assess whether the process of equilibrium dialysis had any effect on GAG content.

As MRE and rheometry provided frequency dependent mechanical properties, the time dependent response of NP tissue was assessed by fitting creep and stress relaxation behavior to a 3-parameter (SLS) viscoelastic model consisting of a Kelvin unit in series with a spring.^{28–30} A schematic of the model can be seen in Figure S2. The model predicts the instantaneous and equilibrium deformation through the parameters G_1 (viscous modulus), G_2 (elastic modulus), and η (viscosity). Curve fitting was performed via a custom MATLAB code.

2.5 | Statistical analysis

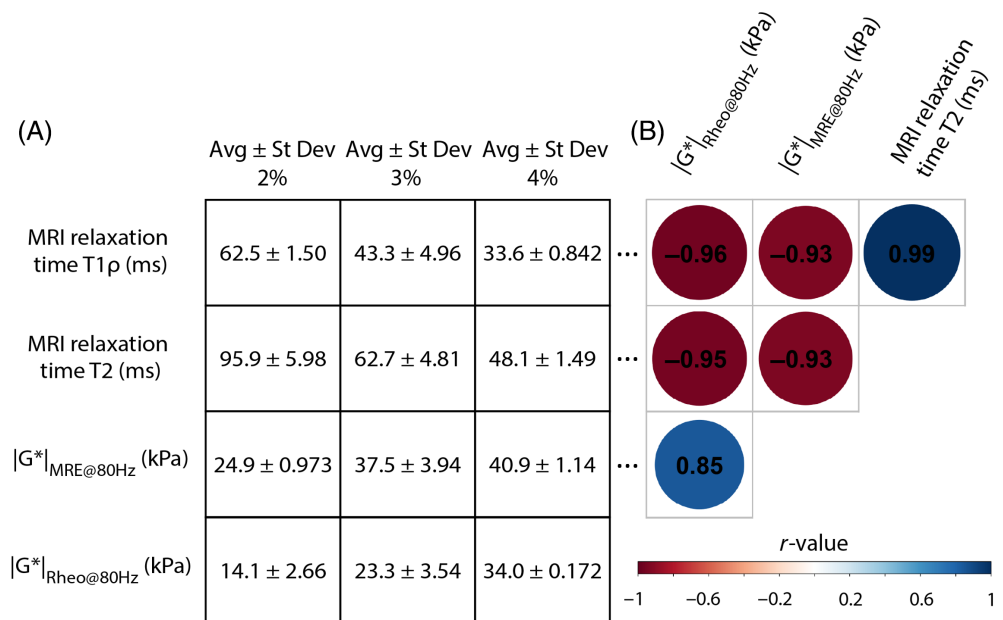
Descriptive summaries of quantitative mechanical properties, MRI parameters, and compositional measures were calculated using the mean and standard deviation. Pearson's correlation was used to summarize the pairwise linear relationship among these experimental factors. Linear mixed-effects models were used to model the complex shear modulus and relaxation time outcomes in agarose and NP tissue. The agarose-based model for complex shear modulus included sample-level random intercepts and fixed effects for method of measurement (MRE or rheometry), percent of agarose, and frequency. We included an interaction between all fixed effects so that the subgroup-specific effect was estimated. The NP tissue-based model for complex shear modulus was similar, using %PEG as a fixed effect and allowing for heteroscedasticity by method of measurement. The relaxation time models included fixed effects for MRI parameter (T1 ρ or T2) and either %agarose or %PEG. For each model, contrasts between the levels of each experimental factor were calculated, and Holm's method was used to adjust the resulting set of *P*-values for multiplicity. Statistical significance was assessed at an alpha level of 0.05. Analyses were performed using R version 4.3.1 and MATLAB version R2018b. R add-on packages included emmeans (version 1.8.8), nlme (version 3.1-162), and lme4 (version 1.1-34).

3 | RESULTS

3.1 | Agarose validation

The MRE-derived and rheometry-derived shear properties were assessed in agarose which provided a controllable, homogenous material. Figure 1A shows T2-weighted image of the agarose with red-dotted lines representing the acquired slices and snapshots of wave images in the x, y, and z directions. MRE-derived magnitude of the complex shear modulus was significantly greater for 4% and 3% samples compared with 2% at 80 Hz (*P* < 0.001) and 100 Hz (*P* < 0.001) (Figure 1B). The mean shear modulus for 4% samples trended higher

FIGURE 2 (A) Mean and standard deviation of MRE- and rheometry-derived mechanical properties and quantitative MRI parameters for 2%, 3%, and 4% agarose groups. (B) Pearson correlations (r) between mechanical properties and MRI parameters. Increasing dot size indicates stronger linear correlation and color the direction of relationship. r -values provided for significant correlations. The y -axis labels for mechanical properties and quantitative MRI parameters in (A) are also used as y -axis labels in (B).



than for 3% at 80 Hz ($P = 0.30$) and at 100 Hz ($P = 0.21$). The magnitude of the mean complex shear modulus increased with frequency for all agarose samples (Figure 1D). Specifically, both imaging and mechanical testing techniques demonstrated higher shear modulus values at 100 Hz compared with 80 Hz (Figure 1B,E). From torsional mechanical testing, 4% samples were significantly stiffer than 3% samples at 80 Hz ($P < 0.001$) and 100 Hz ($P = 0.01$). Shear modulus values for 4% samples were also greater than 2% samples at 80 Hz ($P < 0.001$) and 100 Hz ($P < 0.001$). 3% samples were stiffer than 2% samples at 80 Hz ($P < 0.01$) and 100 Hz ($P = 0.05$) (Figure 1E). Mean values for shear moduli of all agarose percentages at 80 Hz can be seen in Figure 2A. There was a significant positive correlation between shear modulus values obtained via MRE and rheometry at 80 Hz ($r = 0.85$, $P < 0.01$) and at 100 Hz ($r = 0.75$, $P < 0.05$) (Figures 2B and S3). Overall, both MRE and rheometry techniques produced shear modulus values within the same order of magnitude that increased with greater agarose percentage and exhibited the expected frequency dependence as shear modulus increased with frequency.

T1 ρ and T2 relaxation times increased with increasing percentage of agarose (Figure 2A). Univariate correlation analysis showed that T1 ρ correlated significantly with the magnitude of the complex shear modulus derived from MRE at 80 Hz ($|G^*|_{\text{MRE@80Hz}}$) ($r = -0.93$, $P < 0.001$), the magnitude of the complex shear modulus derived from rheometry at 80 Hz ($|G^*|_{\text{Rheometry@80Hz}}$) ($r = -0.96$, $P < 0.001$), and T2 ($r = 0.99$, $P < 0.001$) (Figure 2B). T2 also strongly correlated with MRE-derived ($r = -0.93$, $P < 0.001$) and rheometry-derived ($r = -0.95$, $P < 0.001$) shear modulus measurements at 80 Hz.

3.2 | Tissue validation

Figure 3A shows the magnitudes images of 5% and 25% PEG equilibrated samples with red dotted lines representing the acquired slices

and the snapshot of wave images in one of the samples in all three directions. MRE-derived measurements of the magnitude of the complex shear modulus were significantly greater for 25% PEG equilibrated samples to 5% samples at 80 Hz ($P < 0.001$) and 100 Hz ($P < 0.001$) (Figure 3B). The magnitude of the mean complex shear modulus increased with frequency for all NP samples (Figure 3D). Mean shear modulus values were greater at 100 Hz compared with that at 80 Hz for both imaging and mechanical testing techniques (Figure 3B,E). From torsional mechanical testing, 25% samples were stiffer than 5% samples at both 80 Hz ($P < 0.01$) and 100 Hz ($P < 0.001$) (Figure 3E). Mean values for shear moduli of 5% and 25% PEG equilibrated tissue at 80 Hz can be seen in Figure 4A. There was little correlation between shear modulus values derived from MRE and rheometry at 80 Hz ($r = -0.16$) and at 100 Hz ($r = 0.32$) (Figures 4B and S4). Overall, both MRE and rheometry techniques demonstrated that less hydrated 25% PEG equilibrated NP samples were stiffer, and both exhibited the expected frequency dependence as shear modulus increased with frequency.

Composition of NP tissue was assessed by measuring the %water content and GAG content normalized to dry and wet weight. Additionally, the GAG content from the NP of freshly isolated non-equilibrated IVDs was also assessed and had an average GAG/dry weight of 560 ± 77.7 $\mu\text{g}/\text{mg}$ and average GAG/wet weight of 73.0 ± 11.6 $\mu\text{g}/\text{mg}$. The 5% PEG samples significantly had higher water content than 25% PEG samples ($P < 0.001$) (Figure 4A). The 5% PEG samples had significantly less GAG content per dry weight ($P < 0.001$) and GAG content per wet weight ($P < 0.001$) than 25% samples. T2 and T1 ρ mapping were also performed to get MRI-based measurements that have been demonstrated to correlate with water and GAG content, respectively. T2 ($P < 0.001$) and T1 ρ ($P < 0.001$) relaxation times were significantly greater for the more hydrated 5% PEG samples. Univariate correlation analysis (Figure 4B) showed that GAG content normalized to wet weight significantly correlated with all other measures with the strongest correlations with %water content

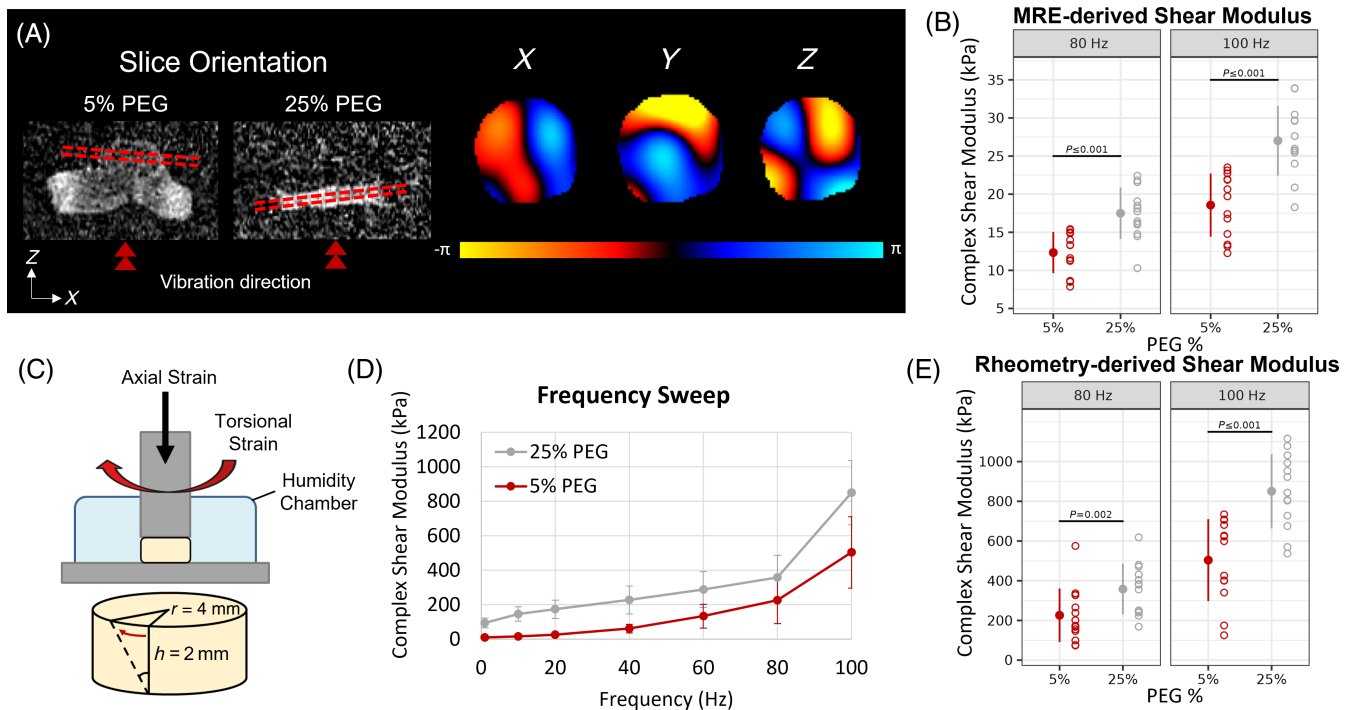
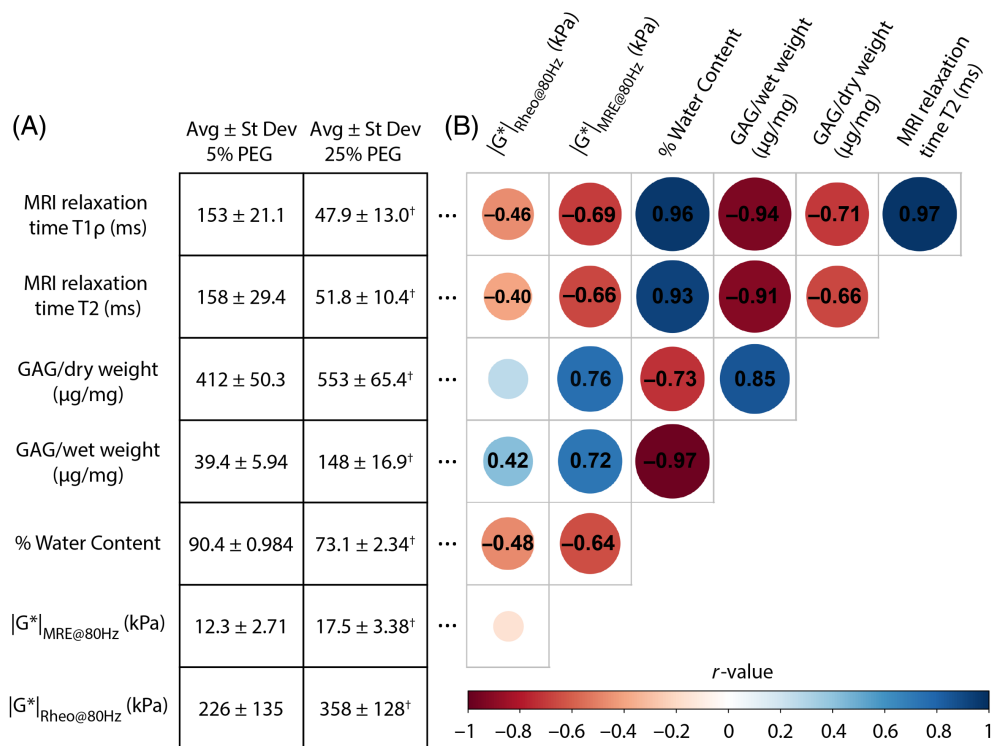


FIGURE 3 Nucleus pulposus (NP) shear properties validation: (A) Schematic of slice orientation through T2-weighted scan of a 5% and 25% PEG equilibrated NP sample with wave directions in the x, y, and z direction. (B) Comparison of shear modulus derived from MRE between 5% ($n = 13$) and 25% ($n = 13$) NP tissue at 80 and 100 Hz. (C) Schematic of NP sample undergoing torsional shear testing using a rheometer. (D) Dynamic frequency sweep results for all NP samples at a shear strain amplitude of $\gamma_0 = 0.05\%$ at frequencies ranging between 1 to 100Hz. (E) Comparison of shear modulus derived from rheometry between all NP samples at 80 and 100 Hz.



($r = -0.97$, $P < 0.001$), T1 ρ ($r = -0.94$, $P < 0.001$), and T2 ($r = -0.91$, $P < 0.001$). It was also positively correlated with $|G^*|_{\text{MRE@80Hz}}$ ($r = 0.72$, $P < 0.001$) and $|G^*|_{\text{Rheometry@80Hz}}$ ($r = 0.42$, $P < 0.05$). GAG

content normalized to dry weight was significantly correlated with T1 ρ ($r = -0.71$, $P < 0.001$), T2 ($r = -0.66$, $P < 0.001$), and $|G^*|_{\text{MRE@80Hz}}$ ($r = -0.76$, $P < 0.001$). In addition to its strong

correlation with GAG content per wet weight, %water content strongly correlated with T2 ($r = 0.93$, $P < 0.001$) and T1 ρ ($r = 0.96$, $P < 0.001$). It was also significantly correlated with $|G^*|_{\text{MRE@80Hz}}$ ($r = -0.64$, $P < 0.001$) and $|G^*|_{\text{Rheometry@80Hz}}$ ($r = -0.48$, $P < 0.05$). T1 ρ correlated significantly with $|G^*|_{\text{MRE@80Hz}}$ ($r = -0.69$, $P < 0.001$) and $|G^*|_{\text{Rheometry@80Hz}}$ ($r = -0.46$, $P < 0.05$) and strongly correlated with T2 ($r = 0.97$, $P < 0.001$). T2 correlated significantly with $|G^*|_{\text{MRE@80Hz}}$ ($r = -0.66$, $P < 0.001$) and $|G^*|_{\text{Rheometry@80Hz}}$ ($r = -0.40$, $P < 0.05$).

Focusing on the modeling parameters obtained via creep and stress relaxation of NP tissue in shear, the elastic and viscous modulus (G_1 , G_2) was greater for 25% PEG equilibrated NP tissue compared with 5% tissue. In addition, the viscosity (η) of 25% tissue was greater than that of 5% tissue (Figure 5A). These findings are consistent with the understanding that less hydrated samples would be stiffer and have a greater resistance to flow. Univariate correlation analysis was performed focusing specifically on the correlations between composition and the modeling parameters (Figure 5B). Creep and stress relaxation model parameters were positively correlated with GAG content normalized to wet weight ($r > 0.73$, $P < 0.001$) and were also positively correlated with GAG content normalized to dry weight ($r > 0.50$, $P < 0.01$) while %water content was negatively correlated

with all viscoelastic modeling parameters ($r < -0.76$, $P < 0.001$). Both T1 ρ and T2 had significant negative correlations with all viscoelastic modeling parameters ($r < -0.68$, $P < 0.001$). Representative creep and stress relaxation responses with the corresponding SLS model fits are shown in Figure S5. Overall, the average R^2 for creep testing for all NP samples was 0.96 ± 0.02 , and the average RMSE was 0.002 ± 0.002 kPa. The average R^2 for stress relaxation testing for all NP samples was 0.92 ± 0.03 , and the average RMSE was 0.08 ± 0.08 kPa.

4 | DISCUSSION

This study aimed to (1) compare MRE-derived and rheometry-derived shear modulus in homogenous agarose gels and heterogenous bovine NP tissue and (2) correlate MRE and rheological measures of NP tissue with composition and quantitative MRI. A spectrum of hydrated agarose samples and hydrated NP tissue were created to assess a range of shear properties. Results demonstrated that both MRE and rheometry derived shear moduli increased in NP tissue and agarose samples with lower water content, and both MRE and rheometry measurements demonstrated a frequency dependence with shear modulus increasing with increasing frequency. However, despite a strong correlation between MRE and rheometric shear measurements present in agarose, there was little correlation between MRE and rheometry in NP tissue demonstrating that MRE can provide a relative assessment of NP tissue shear properties. Comparing the mechanical properties from both techniques with measures of composition and quantitative MRI metrics demonstrated positive correlations with water content and negative correlations with GAG/wet weight, T1 ρ , and T2. Collectively, results suggest MRE measurements of shear mechanical behaviors can inform the structure-function relationship of the IVD.

Altering NP tissue hydration resulted in a change in shear properties as 25% PEG equilibrated NP tissue with lower %water content exhibited greater shear modulus values. A study comparing the shear modulus of normal and severely degenerated human lumbar NP tissue observed similar findings where degenerated tissue demonstrated lower water content and higher modulus values.¹⁹ The complex shear modulus values from this study were within a similar range to past studies. For example, the rheometry-derived complex shear modulus of 5% PEG samples from this study had an average modulus of 10.0 ± 3.2 kPa at 1 Hz, 16.6 ± 5.2 kPa at 10 Hz, and 25.8 ± 7.6 kPa at 20 Hz which are similar to those previously reported for non-degenerate human lumbar NP⁴; 11.3 ± 17.9 kPa at 1 rad/s (~ 0.2 Hz) and 19.8 ± 31.4 kPa at 100 rad/s (~ 15.9 Hz). This study is the first to extend the range of frequency sweep testing to 100 Hz allowing for the comparison between MRE-derived and rheometry-derived shear moduli of NP tissue at similar frequencies. Average MRE-derived measurements of 12.3 ± 2.7 kPa for 5% PEG samples and 17.5 ± 3.4 kPa for 25% PEG samples at 80 Hz were of a similar range to in vivo MRE-derived measurements at varying degeneration levels at the same frequency from prior literature.^{15,16}

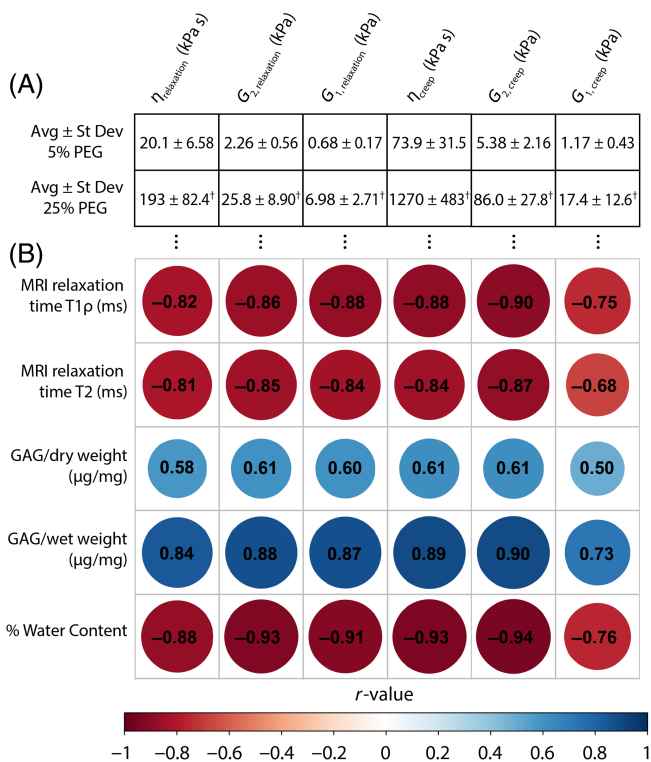


FIGURE 5 (A) Mean and standard deviation of model parameters for creep and stress relaxation for 5% PEG and 25% equilibrated NP tissue. [†] $P < 0.05$ compared against 5% PEG samples. (B) Pearson correlations (r) between model parameters, quantitative MRI parameters, and compositional measures. Increasing dot size indicates stronger linear correlation and color the direction of relationship. r -values provided for significant correlations. The x-axis labels for model parameters in (A) are also used as x-axis labels in (B).

From univariate regression analysis, multiple parameters were identified that were significantly correlated with shear mechanical behaviors (Figures 4 and 5). Specifically, GAG content normalized to wet weight was positively correlated with shear mechanical properties (i.e., MRE- and rheometry-derived shear modulus and creep and stress relaxation parameters), and %water content was negatively correlated with shear properties. The changes observed between water content and shear modulus are consistent with prior work which characterized torsional shear behaviors of human NP tissue from a range of degenerated IVDs and found that more degenerated samples with a lower %water content had a higher shear elastic modulus.¹⁹ Interestingly, multiple studies have evaluated the relationship between composition and mechanical behaviors in compression and found that measures of water content did not significantly correlate with compressive mechanical properties.^{2,21} This difference in correlations between mechanical behaviors of different loading modes with water content emphasizes that water content may more directly inform shear behaviors. A potential mechanism underpinning this relationship is that in shear, fluid flow effects (i.e., poroelastic behaviors) are minimal due to negligible volume changes. Therefore, dynamic responses are primarily driven by interactions between the solid components with the water acting similar to a lubricant influencing the spacing between solid components and, consequently, the number and strength of connections. A similar role has been observed and proposed in rheological behaviors of proteoglycan solutions in which samples with greater proteoglycan concentration (i.e., lower water content) facilitated a greater number of interactions between the solid components and resulted in higher shear moduli.³¹ In compression, the water content itself may be less directly informative of mechanical behaviors which are primarily dominated by the ability of fluid flowing through the solid. It is also notable that we observed a very high correlation between T2 relaxation time and %water content ($r = 0.93$) and correlations between T2 and shear mechanical parameters were very similar to those between %water content and shear properties. The correlation between T2 relaxation time and %water content has been previously demonstrated by many groups and is expected based on MR physics.^{21,32} Collectively, our results, literature, and the understanding of how water contributes to shear responses suggest that T2 relaxation time may more directly inform shear mechanical behavior as compared with compression.

An interesting finding from the univariate regression analysis was that T1 ρ had a significant negative correlation with GAG content—a finding that was consistent with those observed between T1 ρ and GAG content in articular cartilage^{33–36} but opposite from those observed in the IVD.^{22,37} Fundamentally, the T1 ρ parameter describes the spin-lattice relaxation by locking the spins in the rotating frame and captures the interactions between water molecules (i.e., spins) and their local macromolecular environment³⁸ which, in the tissue, is predominately the interaction between water and the extracellular matrix. In particular, T1 ρ measurements are sensitive to how the extracellular matrix restricts the motion of surrounding water molecules when they are locked by a constant radiofrequency energy that is being applied.³⁹ In this study, equilibrium dialysis alters both the amount of free water within the tissue and the density of the solid

matrix (i.e., likely altering how the extracellular matrix constricts the water within the tissue) which is most clearly reflected in the solid-to-fluid ratio or hydration (g water/g dry weight). For example, water was extracted from the 25% PEG equilibrated tissue resulting in less free water molecules within the tissue while becoming more restricted as the tissue was condensed (hydration: 2.8 ± 0.3 g water/g dry weight). The opposite occurred for the 5% PEG equilibrated tissue as the tissue was allowed to imbibe water resulting in more water molecules and the spreading out of macromolecules (hydration: 9.6 ± 1.2 g water/g dry weight). Another interacting factor that may contribute to the similar correlation between T1 ρ and GAG content in our system and that seen in cartilage is that the volume of the NP tissue was able to expand/contract uninhibited by the physical constraints imposed by the endplates (which would limit both expansion and contraction). These conditions are more like articular cartilage in which the tissue is not as physically confined and is able to swell more freely primarily limited by collagen tension. Collectively, our findings reinforce the understanding that T1 ρ is reflective of the interactions between GAG and surrounding water molecules and that while general correlations of T1 ρ with GAG content are relevant within their respective tissues, they are often overly simplistic. Additionally, T1 ρ may be influenced by other macromolecules such as collagen and could be dependent on its orientation/organization. Other degenerative changes such as fibrosis or cross-linking have also been suggested to influence this interaction.^{22,40,41} This finding may elucidate the minor differences in structure or composition that occur during early or late-stage degeneration between IVD and articular cartilage.

4.1 | Limitations

There are a few limitations in this study. The GAG content (both GAG/dry weight and GAG/wet weight) reported in this study is higher than previously reported for bovine NP tissue.⁴⁰ To ensure that the equilibrium dialysis technique was not altering GAG, we assessed the GAG content from NP tissue of three freshly isolated non-equilibrated IVDs. The GAG content from the fresh NP was found to be within the range reported for 5% and 25% equilibrated discs collectively supporting the conclusion that equilibrium dialysis did not influence GAG content. The difference in GAG content in comparison with Mwale et al. may be related to differences in DMMB protocols where Mwale used an earlier iteration of the DMMB protocol⁴² that is less sensitive than the more recently refined method used here.²⁷ Two separate SE-EPI sequences were utilized (SE-EPI_i and SE-EPI_m) to scan either individual IVDs or multiple IVDs simultaneously. The main difference between the two sequences was the slice orientation relative to individual or multiple IVDs. The switch from SE-EPI_i to SE-EPI_m was driven by the desire to reduce scan time as the SE-EPI_m sequence reduced the amount of scan time by a factor of 4. No major differences between shear modulus values obtained by the SE-EPI sequences were observed, and the results from the two sequences were combined. The application of MRE on small regions of interest can impact the ability to accurately estimate the wavelength. To address this limitation, multiple slices through each IVD

were obtained and at least half of the wavelength (Figure 3A) could be seen within the IVD region to report the robust stiffness estimates. Additionally, the PFA inversion algorithm was chosen because it is known to be more robust to noise than other methods as it is performed in the frequency space; however, it provides only a single global modulus value for the entire ROI. Further investigation into other inversion algorithms applicable for small regions of interest is needed to provide spatial stiffness maps.

Although there was a strong correlation between MRE-derived and rheometry-derived shear modulus in agarose, there was little correlation in tissue. We believe inertial effects may have contributed to high rheometry-derived values of tissue due to the geometric limitations of isolating samples from the tissue. Samples with a large diameter and small thickness generally minimize inertial effects on calculated shear properties for torsional testing. This was confirmed by preliminary rheometer testing performed on 2% agarose samples of both 8 mm and 20 mm diameter where the shear modulus values for the 8 mm diameter samples were an order of magnitude higher than the 20 mm diameter samples values reported in this study (80 Hz: $|G^*|_{2\% \text{ Agarose}, 8 \text{ mm} \varnothing} = 261 \pm 118 \text{ kPa}$ and $|G^*|_{2\% \text{ Agarose}, 20 \text{ mm} \varnothing} = 14.1 \pm 2.66 \text{ kPa}$). For agarose, there was no size limitation of samples and larger 20 mm diameter samples were used; however, the largest diameter possible from bovine NP tissue was 8 mm. Additionally, the minimum thickness for NP tissue that could be reproducibly obtained via cryo-sectioning was 2 mm; collectively limiting the dimensions of NP tissue to 8 mm $\varnothing \times$ 2 mm thick plugs. Additionally, the inhomogeneity and animal-to-animal variation of biological tissue may also have contributed. Despite smaller sample geometry, data from rheometry still demonstrated the same frequency dependence as seen with MRE and clearly showed that it was able to detect differences between 5% and 25% PEG groups.

5 | CONCLUSION

Overall, results in both agarose and IVD tissue demonstrated that MRE and rheometry can detect differences in shear properties with changes in hydration. Both techniques provided relative measures of frequency-dependent shear modulus and demonstrated that decreasing water content increases the agarose or tissue shear “stiffness.” Our results further demonstrated that composition, such as water content and GAG content, play an important role in the mechanical function of NP tissue. Second, MR imaging metrics (T1 ρ and T2 relaxation times) that have primarily been used to assess composition within IVD tissue also correlated with shear mechanical properties and may further inform mechanics of the tissue. Collectively, this study demonstrated that MRE-derived shear properties of IVD tissue aids in explaining the complex relationship between structure and function within IVDs in shear.

ACKNOWLEDGMENTS

We would like to acknowledge Dr. Aleksander Skardal for the use of the rheometer and helpful technical conversations. We also acknowledge Zachary Osborn-King for his assistance in conducting and

optimizing the DMMB protocol used. Research reported in this publication was supported by the Department of Biomedical Engineering at The Ohio State University, the National Institute of Arthritis and Musculoskeletal and Skin Diseases (Award Number R01AR075062). The content is solely the responsibility of the authors and does not necessarily represent the official views of the National Institutes of Health.

CONFLICT OF INTEREST STATEMENT

The authors declare no conflicts of interest.

FUNDING INFORMATION

This manuscript has been supported by grant sponsor: NIH-NIAMS; Grant number: R01AR075062.

ORCID

Benjamin Walter  <https://orcid.org/0000-0002-0742-5533>

REFERENCES

1. Ferreira ML, de Luca K, Haile LM, et al. Global, regional, and national burden of low back pain, 1990–2020, its attributable risk factors, and projections to 2050: a systematic analysis of the Global Burden of Disease Study 2021. *Lancet Rheumatol*. 2023;5:e329. doi:10.1016/S2665-9913(23)00098-X
2. Johannessen W, Elliott DM. Effects of degeneration on the biphasic material properties of human nucleus pulposus in confined compression. *Spine (Phila Pa 1976)*. 2005;30(24):E724-E729. doi:10.1097/01.brs.0000192236.92867.15
3. Acaroglu ER, Iatridis JC, Setton LA, Foster RJ, Mow VC, Weidenbaum M. Degeneration and aging affect the tensile behavior of human lumbar annulus fibrosus. *Spine (Phila Pa 1976)*. 1995;20:2690-2701.
4. Iatridis JC, Setton LA, Weidenbaum M, Mow VC. The viscoelastic behavior of the non-degenerate human lumbar nucleus pulposus in shear. *J Biomech*. 1997;30:1005-1013. doi:10.1016/S0021-9290(97)00069-9
5. Iatridis JC, Setton LA, Foster RJ, Rawlins BA, Weidenbaum M, Mow VC. Degeneration affects the anisotropic and nonlinear behaviors of human annulus fibrosus in compression. *J Biomech*. 1998;31:535-544. doi:10.1016/S0021-9290(98)00046-3
6. Venkatesh SK, Yin M, Ehman RL. Magnetic resonance elastography of liver: technique, analysis, and clinical applications. *J Magn Reson Imaging*. 2013;37:544-555. doi:10.1002/jmri.23731
7. Chamrathi SK, Raterman B, Mazumder R, et al. Rapid acquisition technique for MR elastography of the liver. *Magn Reson Imaging*. 2014;32:679-683. doi:10.1016/j.mri.2014.02.013
8. Kolipaka A, Araoz PA, McGee KP, Manduca A, Ehman RL. Magnetic resonance elastography as a method for the assessment of effective myocardial stiffness throughout the cardiac cycle. *Magn Reson Med*. 2010;64(3):862-870. doi:10.1002/mrm.22467
9. Kolipaka A, Illapani VSP, Kenyhercz W, et al. Quantification of abdominal aortic aneurysm stiffness using magnetic resonance elastography and its comparison to aneurysm diameter. *J Vasc Surg*. 2016;64:966-974. doi:10.1016/j.jvs.2016.03.426
10. Simon M, Guo J, Papazoglou S, et al. Non-invasive characterization of intracranial tumors by magnetic resonance elastography. *New J Phys*. 2013;15:15. doi:10.1088/1367-2630/15/8/085024
11. Streitberger KJ, Diederichs G, Guo J, et al. In vivo multifrequency magnetic resonance elastography of the human intervertebral disk. *Magn Reson Med*. 2015;74:1380-1387. doi:10.1002/mrm.25505
12. Cortes DH, Magland JF, Wright AC, Elliott DM. The shear modulus of the nucleus pulposus measured using magnetic resonance

- elastography: a potential biomarker for intervertebral disc degeneration. *Magn Reson Med*. 2014;72:211-219. doi:[10.1002/mrm.24895](https://doi.org/10.1002/mrm.24895)
13. Ben-Abraham EI, Chen J, Felmlee JP, et al. Feasibility of MR elastography of the intervertebral disc. *Magn Reson Imaging*. 2017;39:132-137. doi:[10.1016/j.mri.2015.12.037](https://doi.org/10.1016/j.mri.2015.12.037)
 14. Beauchemin PF, Bayly PV, Garbow JR, et al. Frequency-dependent shear properties of annulus fibrosus and nucleus pulposus by magnetic resonance elastography. *NMR Biomed*. 2018;31(10):1-8. doi:[10.1002/nbm.3918](https://doi.org/10.1002/nbm.3918)
 15. Walter BA, Boulter DJ, Thoman W, Raterman BD, Rt R, Mendel E. MRI elastography-derived stiffness: a biomarker for intervertebral disc degeneration 1. *Radiology*. 2017;285(1):167-175.
 16. Co M, Dong H, Boulter DJ, et al. Magnetic resonance elastography of intervertebral discs: spin-echo echo-planar imaging sequence validation. *J Magn Reson Imaging*. 2022;56:1722-1732. doi:[10.1002/jmri.28151](https://doi.org/10.1002/jmri.28151)
 17. Klatt D, Friedrich C, Korth Y, Vogt R, Braun J, Sack I. Viscoelastic properties of liver measured by oscillatory rheometry and multifrequency magnetic resonance elastography. *Biorheology*. 2010;47(2):133-141. doi:[10.3233/BIR-2010-0565](https://doi.org/10.3233/BIR-2010-0565)
 18. Antoniou J, Epure LM, Michalek AJ, Grant MP, Iatridis JC, Mwale F. Analysis of quantitative magnetic resonance imaging and biomechanical parameters on human discs with different grades of degeneration. *J Magn Reson Imaging*. 2013;38:1402-1414. doi:[10.1002/jmri.24120](https://doi.org/10.1002/jmri.24120)
 19. Iatridis JC, Setton LA, Weidenbaum M, Mow VC. Alterations in the mechanical behavior of the human lumbar nucleus pulposus with degeneration and aging. *J Orthop Res*. 1997;15:318-322. doi:[10.1002/jor.1100150224](https://doi.org/10.1002/jor.1100150224)
 20. Boxberger JI, Orlansky AS, Sen S, Elliott DM. Reduced nucleus pulposus glycosaminoglycan content alters intervertebral disc dynamic viscoelastic mechanics. *J Biomech*. 2009;42(12):1941-1946. doi:[10.1016/j.jbiomech.2009.05.008](https://doi.org/10.1016/j.jbiomech.2009.05.008)
 21. Gullbrand SE, Ashinsky BG, Martin JT, et al. Correlations between quantitative T2 and T1p MRI, mechanical properties and biochemical composition in a rabbit lumbar intervertebral disc degeneration model. *J Orthop Res*. 2016;34(8):1382-1388. doi:[10.1002/jor.23269](https://doi.org/10.1002/jor.23269)
 22. Nguyen AM, Johannessen W, Yoder JH, et al. Noninvasive quantification of human nucleus pulposus pressure with use of T1p-weighted magnetic resonance imaging. *J Bone Jt Surg Ser A*. 2008;90:796-802. doi:[10.2106/JBJS.G.00667](https://doi.org/10.2106/JBJS.G.00667)
 23. Chahine NO, Chen FH, Hung CT, Ateshian GA. Direct measurement of osmotic pressure of glycosaminoglycan solutions by membrane osmometry at room temperature. *Biophys J*. 2005;89(3):1543-1550. doi:[10.1529/biophysj.104.057315](https://doi.org/10.1529/biophysj.104.057315)
 24. Iatridis JC, Weidenbaum M, Setton LA, Mow VC. Is the nucleus pulposus a solid or a fluid? Mechanical behaviors of the nucleus pulposus of the human intervertebral disc. *Spine (Phila Pa 1976)*. 1996;21(10):1174-1184.
 25. Gandhi D, Kalra P, Raterman B, Mo X, Dong H, Kolipaka A. Magnetic resonance elastography of kidneys: SE-EPI MRE reproducibility and its comparison to GRE MRE. *NMR Biomed*. 2019;32(11):1-11. doi:[10.1002/nbm.4141](https://doi.org/10.1002/nbm.4141)
 26. McGee KP, Lake D, Mariappan Y, et al. Calculation of shear stiffness in noise dominated magnetic resonance elastography (MRE) data based on principal frequency estimation. *Phys Med Biol*. 2011;56(14):4291-4309. doi:[10.1088/0031-9155/56/14/006](https://doi.org/10.1088/0031-9155/56/14/006)
 27. Zheng C, Levenston M. Fact versus artifact: avoiding erroneous estimates of sulfated glycosaminoglycan content using the dimethylmethylene blue colorimetric assay for tissue-engineered constructs. *Eur Cells Mater*. 2015;29:224-236. doi:[10.22203/eCM.v029a17](https://doi.org/10.22203/eCM.v029a17)
 28. Keller TS, Spengler DM, Hansson TH. Mechanical behavior of the human lumbar spine. I. Creep analysis during static compressive loading. *J Orthop Res*. 1987;5(4):467-478. doi:[10.1002/jor.1100050402](https://doi.org/10.1002/jor.1100050402)
 29. Kaleps I, Kazarian LE, Burns ML. Analysis of compressive creep behavior of the vertebral unit subjected to a uniform axial loading using exact parametric solution equations of kelvin-solid models-part II. Rhesus monkey intervertebral joints. *J Biomech*. 1984;17(2):131-136. doi:[10.1016/0021-9290\(84\)90130-1](https://doi.org/10.1016/0021-9290(84)90130-1)
 30. Pollintine P, Van Tunen MSLM, Luo J, Brown MD, Dolan P, Adams MA. Time-dependent compressive deformation of the ageing spine: relevance to spinal stenosis. *Spine (Phila Pa 1976)*. 2010;35(4):386-394. doi:[10.1097/BRS.0b013e3181b0ef26](https://doi.org/10.1097/BRS.0b013e3181b0ef26)
 31. Mow VC, Zhu W, Lai WM, Hardingham TE, Hughes C, Muir H. The influence of link protein stabilization on the viscometric properties of proteoglycan aggregate solutions. *Biochem Biophys Acta*. 1989;992:201-208.
 32. Marinelli NL, Houghton VM, Muñoz A, Anderson PA. T2 relaxation times of intervertebral disc tissue correlated with water content and proteoglycan content. *Spine (Phila Pa 1976)*. 2009;34(5):520-524. doi:[10.1097/BRS.0b013e318195dd44](https://doi.org/10.1097/BRS.0b013e318195dd44)
 33. Wheaton AJ, Dodge GR, Elliott DM, Nicoll SB, Reddy R. Quantification of cartilage biomechanical and biochemical properties via T1p magnetic resonance imaging. *Magn Reson Med*. 2005;54(5):1087-1093. doi:[10.1002/mrm.20678](https://doi.org/10.1002/mrm.20678)
 34. Akella SVS, Regatte RR, Gougoutas AJ, et al. Proteoglycan-induced changes in T1p-relaxation of articular cartilage at 4T. *Magn Reson Med*. 2001;46(3):419-423. doi:[10.1002/mrm.1208](https://doi.org/10.1002/mrm.1208)
 35. Regatte RR, Akella SVS, Borthakur A, Kneeland JB, Reddy R. Proteoglycan depletion-induced changes in transverse relaxation maps of cartilage: comparison of T2 and T1p. *Acad Radiol*. 2002;9(12):1388-1394. doi:[10.1016/S1076-6332\(03\)80666-9](https://doi.org/10.1016/S1076-6332(03)80666-9)
 36. Keenan KE, Besier TF, Pauly JM, et al. Prediction of glycosaminoglycan content in human cartilage by age, T1p and T2 MRI. *Osteoarthr Cartil*. 2011;19(2):171-179. doi:[10.1016/j.joca.2010.11.009](https://doi.org/10.1016/j.joca.2010.11.009)
 37. Johannessen W, Auerbach JD, Wheaton AJ, et al. Assessment of human disc degeneration and proteoglycan content using T1p-weighted magnetic resonance imaging. *Spine (Phila Pa 1976)*. 2006;31:1253-1257. doi:[10.1097/01.brs.0000217708.54880.51](https://doi.org/10.1097/01.brs.0000217708.54880.51)
 38. Redfield AG. Nuclear spin thermodynamics in the rotating frame. *Science*. 1969;164(3883):1015-1023. doi:[10.1126/science.164.3883.1015](https://doi.org/10.1126/science.164.3883.1015)
 39. Li X, Benjamin Ma C, Link TM, et al. In vivo T1p and T2 mapping of articular cartilage in osteoarthritis of the knee using 3 T MRI. *Osteoarthr Cartil*. 2007;15(7):789-797. doi:[10.1016/j.joca.2007.01.011](https://doi.org/10.1016/j.joca.2007.01.011)
 40. Mwale F, Demers CN, Michalek AJ, et al. Evaluation of quantitative magnetic resonance imaging, biochemical and mechanical properties of trypsin-treated intervertebral discs under physiological compression loading. *J Magn Reson Imaging*. 2008;27:563-573. doi:[10.1002/jmri.21242](https://doi.org/10.1002/jmri.21242)
 41. Menezes NM, Gray ML, Hartke JR, Burstein D. T2 and T1p MRI in articular cartilage systems. *Magn Reson Med*. 2004;51(3):503-509. doi:[10.1002/mrm.10710](https://doi.org/10.1002/mrm.10710)
 42. Farndale R, Buttle D, Barrett A. Improved quantitation and discrimination of sulphated glycosaminoglycans by use of dimethylmethylene blue. *Biochim Biophys Acta - Gen Subj*. 1986;883(2):173-177. doi:[10.1016/0304-4165\(86\)90306-5](https://doi.org/10.1016/0304-4165(86)90306-5)

SUPPORTING INFORMATION

Additional supporting information can be found online in the Supporting Information section at the end of this article.

How to cite this article: Co M, Raterman B, Klamer B, Kolipaka A, Walter B. Nucleus pulposus structure and function assessed in shear using magnetic resonance elastography, quantitative MRI, and rheometry. *JOR Spine*. 2024;7(2):e1335. doi:[10.1002/jsp2.1335](https://doi.org/10.1002/jsp2.1335)